# Two-Fluid Model for Particle-Turbulence Interaction in a Backward-Facing Step

**K. Mohanarangam and J. Y. Tu**
School of Aerospace, Mechanical and Manufacturing Engineering, RMIT University, Vic. 3083, Australia

*DOI 10.1002/aic.11248*
*Published online July 25, 2007 in Wiley InterScience (www.interscience.wiley.com).*

*Particle-turbulence interaction for dilute gas-particle flows over a backward-facing step geometry is numerically investigated. An Eulerian two-fluid model with additional turbulence transport equations for particles is employed in this investigation. RNG based k-ε model is used as the turbulent closure with additional transport equations solved, to better represent the combined gas-particle interactions. Two different particle classes with same Stokes number and varied particle Reynolds number are considered in this study. The turbulence modulation of the carrier phase in the presence of the dispersed particulate phase is simulated and compared against the experimental data. However prior to this endeavour, the simulated flow field is validated for mean streamwise velocities and fluctuations for both the phases. Despite the fact that the two particles used in this study share the same Stokes number their behavior is found to be considerably different in the turbulent flow field, which basically underlines the fact that the Stokes number alone is not enough to fully describe the behavior of particles, thereby, herein particle Reynolds number is also investigated to fully understand their behavior. Two other turbulence modulation models were also tested against our own formulation, and our model was found to compare better with the experimental findings.* © 2007 American Institute of Chemical Engineers *AIChE J,* 53: 2254–2264, 2007
*Keywords: dilute gas-particle flows, backward-facing step, Eulerian two-fluid model, turbulence modulation, particle Reynolds number*

## Introduction

The basics of gas-particle flows have received interdisciplinary attention from chemical, mechanical and industrial engineers for decades as they play a major role in a variety of industrial and design processes. Computational fluid dynamics (CFD) have gone a long way to describe these processes, which of course, without any doubt, is not only, the most potent and cost-effective way to understand the hydrodynamics of gas-particle flows, but also provides the user with the potential to analyze on a fundamental basis. With increasing computational power, numerical simulation has become an indispensable tool to study fluid dynamics and heat transfer in multiphase flows.[1]

Dilute gas-particle flows are encountered in wide range of natural, industrial and engineering applications. Their presence range from the dispersion of spores by certain species of plants, dust encountered in our living rooms to that of the pulverised coal combustion and solid transport equipments, used in industries. In industrial and engineering applications a better understanding of the physics of these flows will not only lead to better operating efficiency by improved equipment designs, but also increase the longevity accompanied with lower maintenance costs and better operational improvements.

Previous studies have shown that the addition of solid or liquid particles to a turbulent flow, at volume fractions of $10^{-5}$ have shown to modify the structure of turbulence, and also alter the transport rates of momentum and mass and this

Correspondence concerning this article should be addressed to J. Y. Tu at jiyuan.tu@rmit.edu.au.

modification of the carrier phase will directly affect the dispersion of the dispersed phase, thereby rendering a two-way interaction effect.[2] Gore and Crowe[3] tabulated the available experimental data on the turbulent modulation in particle-laden flows, their study is based on the proposed critical parameter $d/l$, where $d$ is the diameter of the dispersed phase, and $l$ is the Eulerian integral length scale of turbulence. Their classification based on proposed critical parameter that predicts whether turbulence will be augmented or suppressed has a critical value of $\sim$0.1, above which the turbulence intensity is increased, else otherwise. Fessler and Eaton[4] found that for a flow with a certain Stokes number for a given particle Reynolds number there is turbulence attenuation with the carrier phase, however, this trend of increasing attenuation cannot continue as Hetsroni[5] has instituted that the particles with Reynolds number greater than 400 will enhance the turbulence of the gas (or carrier) phase flow.

Numerical modeling of these classes of flows poses a problem, considering the diversity of particle-laden flows, wherein the addition of particles to a flow greatly increases the parameter space of the problem. In addition to the complexity involved in tracking the particles, the mere presence of particles can drastically change the characteristics of the flow itself.[6] The turbulent dispersion of these dispersed phase particles within the carrier phase can be studied by two orders, one by presuming that the presence of particles does not have any effect on the turbulent carrier flow field, which is considered to be "one way coupling", and the second by considering a feedback of the presence of particles into the carrier flow field, in addition to the particle getting affected by the carrier flow field, this is considered to be "two-way coupling", which is most of the times the precise phenomena taking place in the real world.

Reynolds-averaged Navier-Stokes equations are one of the well known numerical approaches to predict the turbulence modulation (*TM*) of the carrier phase. They stem out as a consequence of time average to yield the constitutive mean flow equations, however, the turbulent stresses which arise as a direct consequence should be modelled with some degree of approximation. Specification of the turbulent eddy viscosity serves as the turbulent closure, and the $k$-$\varepsilon$ turbulence formulation specifies this by solving two additional transport equations for turbulent kinetic energy and the eddy dissipation. This being the case for single phase flows, for dilute nonreacting particulate flows, these pose a problem in the sense the momentum of the carrier phase undergoes a phenomenal change due to the presence of particles, this is also reflected in terms of TM of the carrier phase. Elghobashi and Abou-Arab[7] rigorously derived the exact transport equations for $k$, and $\varepsilon$ for two-phase dilute particulate flows and obtained reasonable agreement with the experimental results, other varied formulations of $k$-$\varepsilon$ turbulence model for dilute particle laden flows have been proposed (Shuen et al.,[8] Mostafa and Mongia,[9] Chen and Wood,[10] Rizk and Elghobashi,[11] Dasgupta et al.,[12] Bolio et al.[13]). Interestingly Zhou and Chen[14] and Simonin[15] separately proposed the particle Reynolds stress equation and particle turbulent kinetic energy equation, which tends to fall in line with our current formulation, but these models were put to test only to simulate the mean quantities of velocity and fluctuation of the carrier and the particulate phases. In this study our model[16,17] have not only been able to simulate the mean experimental quantities of velocity and fluctuation of the two phases, but also to study the TM of the carrier gas phase in the presence of the particulate phase for two varying particles sharing the same Stokes number but quite different particle Reynolds number.

In addition to this, the long standing issue of whether the addition of a secondary phase like particles causes either an augmentation or attenuation of the carrier phase turbulence is not very well understood. Kenning and Crowe[18] proposed that the turbulence enhancement is caused by the work done by the particles to overcome its drag, and turbulence attenuation is caused by the interparticle spacing restriction, they proposed a model based on the modification of the dissipation length scale to account for the presence of the particles, however, as pointed out by Zhang and Reese[19] who previously tested this model, attribute the use of prescribed turbulence length scale in Kenning and Crowe's model. Later they considered and derived a model based on the interparticle length scale on the gas turbulence based on the experimental results from Sato et al.[20] mentioned earlier.

## Outline of the Article

In this article, we present the TM results of the carrier phase, in the presence of the dispersed particulate phase, for this approach two sets of particle classes viz, 70 $\mu$m copper particles and 150 $\mu$m glass particles (from here referred to as copper and glass particles, respectively) are selected, the reason behind selecting these two classes of particles, is that they share the same Stokes number ($St$), while differing by particle Reynolds number ($Re_p$). We start by introducing the computational model used in this study, followed by the numerical procedure used to obtain the simulation results. Prior to the results and discussion, the code has been validated to replicate the experimental results of the mean streamwise velocity and fluctuation for both the phases.

The results and discussion section starts by experimental analysis of the degree of attenuation caused by the two sets of particles as reported from the experimental findings of Fessler and Eaton[6] behind the backward facing step geometry. Followed by this, TM models of Kenning and Crowe[18] along with Zhang and Reese[19] are numerically tested for the two classes of particles behind the step. Extended results of the TM along with the particle number density (*PND*) results are plotted to ascertain and derive the link of the PND to TM. Finally, we have gone a step further and tried to explain why the larger glass particle attenuate rather than enhance turbulence of the carrier phase in relation to the $Re_p$.

## Computational Model

The Eulerian two-fluid model developed by Tu and Fletcher[16] and Tu[17] used in this study considers the gas and particle phases as two interpenetrating continua. Hereby, a two-way coupling is achieved between the dispersed and the carrier phases.

The underlying assumptions employed in the current study are:

(1) The particulate phase is dilute and consists of mono disperse spherical particles.

(2) For such a dilute flow, the gas volume fraction is approximated by unity.

(3) The viscous stress and the pressure of the particulate phase are negligible.
(4) The flow field is isothermal.

### *Gas phase*

The governing equations in Cartesian form for steady, mean turbulent gas flow are obtained by Favre averaging the instantaneous continuity and momentum equations

$$\frac{\partial}{\partial x_i}(\rho_g u_g^i) = 0 \tag{1}$$

$$\frac{\partial}{\partial x_j}(\rho_g u_g^j u_g^i) = -\frac{\partial p_g}{\partial x_i} + \frac{\partial}{\partial x_j}\left(\rho_g v_{gl}\frac{\partial}{\partial x_j}u_g^i\right) - \frac{\partial}{\partial x_j}(\rho_g \overline{u_g^{\prime j} u_g^{\prime i}}) - F_{Di} \tag{2}$$

$$\frac{\partial}{\partial x_j}(\rho_g u_g^j k_g) = \frac{\partial}{\partial x_j}\left(\alpha\rho_g v_{gt}\frac{\partial k_g}{\partial x_j}\right) + P_{kg} - \rho_g\varepsilon_g + S_k \tag{3}$$

$$\frac{\partial}{\partial x_j}(\rho_g u_g^j \varepsilon_g) = \frac{\partial}{\partial x_j}\left(\alpha\rho_g v_{gt}\frac{\partial \varepsilon_g}{\partial x_j}\right) + \frac{\varepsilon_g}{k_g}(C_{\varepsilon 1}P_{kg} - C_{\varepsilon 2}\rho_g\varepsilon_g) - \rho_g \mathrm{R} + \mathrm{S}_\varepsilon \tag{4}$$

Equations 1 and 2, respectively, are the continuity and momentum equation of the carrier gas phase, where $\rho_g$, $u_g$, $u_g'$ and $p_g$ are the bulk density, mean velocity, fluctuating velocity and mean pressure of the gas phase, respectively. $v_{gl}$ is the laminar viscosity of the gas phase. $F_{Di}$ is the Favre-averaged aerodynamic drag force due to the slip velocity between the two phases and is given by

$$F_{Di} = \rho_p \frac{f(u_g^i - u_p^i)}{t_p} \tag{5}$$

where the correction factor $f$ is selected according to Schuh et al.[21]

$$f = \begin{cases} 1 + 0.15\,Re_p^{0.687} & 0 < Re_p \le 200 \\ 0.914\,Re_p^{0.282} + 0.0135\,Re_p & 200 < Re_p \le 2500 \\ 0.0167\,Re_p & 2500 < Re_p \end{cases} \tag{6}$$

with the particle response or relaxation time given by $t_p = \rho_s d_p^2/(18\rho_g v_{\mathrm{gl}})$, wherein $d_p$ is the diameter of the particle. For the carrier gas phase, which uses an eddy-viscosity model, the Reynolds stresses are given by

$$\rho_g \overline{u_g^{\prime i} u_g^{\prime j}} = -\rho_g v_{gt}\left(\frac{\partial u_g^i}{\partial x_j} + \frac{\partial u_g^j}{\partial x_i}\right) + \frac{2}{3}\rho_g k_g \delta_{ij} \tag{7}$$

where $v_{gt}$ is the turbulent or "eddy" viscosity of the gas phase, which is computed by $v_{gt} = C_\mu\,(k_g^2/\varepsilon_g)$. The kinetic energy of the turbulence, $k_g$ and its dissipation rate, $\varepsilon_g$ is governed by separate transport equations. The RNG theory, models the $k_g$ and $\varepsilon_g$ transport Eqs. 3 and 4, respectively, by taking into account the particulate turbulence modulation, in which $\alpha$ is the inverse Prandtl number. The rate of strain term $R$ in the $\varepsilon_g$-equation is expressed as

$$R = \frac{C_\mu \eta^3(1-\eta/\eta_0)}{1+\beta\eta^3}\frac{\varepsilon_g^2}{k_g}, \quad \eta = \frac{k_g}{\varepsilon_g}(2S_{ij}^2)^{1/2}, \quad S_{ij} = \frac{1}{2}\left(\frac{\partial u_g^{\mathrm{i}}}{\partial x_j} + \frac{\partial u_g^{\mathrm{j}}}{\partial x_{\mathrm{i}}}\right) \tag{8}$$

where $\beta = 0.015$, $\eta_0 = 4.38$. The major endeavour of including this term is to take into account the effects of rapid strain rate along with the streamline curvature, which in many cases the standard $k$-$\varepsilon$ turbulence model fails to predict. The constants in the turbulent transport equations are given by $\alpha = 1.3929$, $C_\mu = 0.0845$, $C_{\varepsilon 1} = 1.42$ and $C_{\varepsilon 2} = 1.68$ as per the RNG theory.[22]

For the confined two-phase flow, the effects of the particulate phase on the turbulence of the gas phase are taken into account through the additional terms $S_k$ and $S_\varepsilon$ in the $k_g$ and $\varepsilon_g$ equations, which arise from the correlation term given by

$$S_k = (\overline{-u_g^{\prime i} F_{Di}^{\prime}}) = -\frac{2f}{t_p}\rho_p(k_g - k_{gp}) \tag{9}$$

in the $k_g$ equation and

$$S_\varepsilon = -2v_{gl}\frac{\overline{\partial u_g^{\prime i}\,\partial F_{Di}^{\prime}}}{\partial x_j \partial x_j} = -\frac{2f}{t_p}\rho_p(\varepsilon_g - \varepsilon_{gp}) \tag{10}$$

in the $\varepsilon_g$ equation, where $k_{gp}$ and $\varepsilon_{gp}$ will be presented in the following section discussing the particulate turbulence modeling.

### *Particulate phase*

After Favre averaging, the steady form of the governing equations for the particulate phase is

$$\frac{\partial}{\partial x_i}(\rho_p u_p^i) = 0 \tag{11}$$

$$\frac{\partial}{\partial x_j}(\rho_p u_p^j u_p^i) = -\frac{\partial}{\partial x_j}\left(\rho_p \overline{u_p^{\prime} j u_p^{\prime} i}\right) + F_{Gi} + F_{Di} + F_{WMi} \tag{12}$$

$$\frac{\partial}{\partial x_j}(\rho_p u_p^j k_p) = \frac{\partial}{\partial x_j}\left(\rho_p \frac{v_{pt}}{\sigma_p}\frac{\partial k_p}{\partial x_j}\right) + P_{kp} - I_{gp} \tag{13}$$

where $\rho_p$, $u_p$ and $u'_p$ are the bulk density, mean and fluctuating velocity of the particulate phase, respectively. In Eq. 12, there are three additional terms representing the gravity force, aerodynamic drag force, and the wall-momentum transfer force due to particle-wall collisions, respectively. The gravity force is $F_{Gi} = \rho_p g$, where $g$ is the gravitational acceleration. The turbulence production $P_{kp}$ of the particulate phase is given by

$$P_{kp} = \rho_p v_{pt}\left(\frac{\partial u_p^i}{\partial x_j} + \frac{\partial u_p^j}{\partial x_i}\right)\frac{\partial u_p^i}{\partial x_k} - \frac{2}{3}\rho_p \delta_{ij}\left(k_p + v_{pt}\frac{\partial u_p^k}{\partial x_k}\right)\frac{\partial u_p^i}{\partial x_k} \tag{14}$$

and the turbulence interaction between two phases $I_{gp}$ is given by

$$I_{gp} = \frac{2f}{t_p}\rho_p(k_p - k_{gp}) \tag{15}$$

Here $k_{gp} = \frac{1}{2}\overline{u_g^{\prime i} u_p^{\prime i}}$ is the turbulence kinetic energy interaction between two phases. The transport equation for the

gas-particle covariance $\overline{u_g'^i u_p'^i}$ can be again derived,[17] to obtain the transport equation governing the gas-particle correlation, which is given by

$$\frac{\partial}{\partial x_j}[\rho_p(u_g^i + u_p^i)k_{gp}] = \frac{\partial}{\partial x_j}\rho_p\left(\frac{\nu_{gt}}{\sigma_g} + \frac{\nu_{pt}}{\sigma_p}\right)\frac{\partial k_{gp}}{\partial x_j} + P_{gp} - \rho_p\varepsilon_{gp} - II_{gp} \quad (16)$$

where the turbulence production by the mean velocity gradients of two phases is

$$P_{gp} = \left\{\rho_p\left(\nu_{gt}\frac{\partial u_g^i}{\partial x_j} + \nu_{pt}\frac{\partial u_p^j}{\partial x_i}\right) - \frac{2}{3}\rho_p\delta_{ij}k_{gp} - \frac{1}{3}\bar{\rho}_p\delta_{ij}\left(\nu_{gt}\frac{\partial u_p^k}{\partial x_k} + \nu_{pt}\frac{\partial u_p^k}{\partial x_k}\right)\right\}\left(\frac{\partial u_g^i}{\partial x_j} + \frac{\partial u_p^i}{\partial x_j}\right) \quad (17)$$

The interaction term between the two phases takes the form

$$II_{gp} = \frac{f}{2t_p}\rho_p[(1+m)2k_{gp} - 2k_g - m2k_p] \quad (18)$$

here $m$ is the mass ratio of the particle to the gas, $m = \rho_p/\rho_g$. The dissipation term due to the gas viscous effect is modeled by

$$\varepsilon_{gp} = \varepsilon_g \exp\left(-B_\varepsilon t_p \frac{\varepsilon_g}{k_g}\right) \quad (19)$$

where

$$B_\varepsilon = 0.4.$$

The turbulent eddy viscosity of the particulate phase $\nu_{pt}$, is defined in a similar way as the gas phase as

$$\nu_{pt} = \frac{2}{3}k_p t_{pt} = \ell_{pt}\sqrt{\frac{2}{3}k_p} \quad (20)$$

The turbulent characteristic length of the particulate phase is modeled by $l_{pt} = \min(l'_{pt}, D_s)$ where $l'_{pt}$ is given by

$$l'_{pt} = \frac{l_{gt}}{2}(1+\cos^2\theta)\exp\left[-B_{gp}\frac{|u'_r|}{|u'_g|}sign(k_g - k_p)\right] \quad (21)$$

where θ is the angle between the velocity of the particle and the velocity of the gas to account for the crossing trajectories effect.[23] $B_{gp}$ is an experimentally determined constant, which takes a value of 0.01. $D_s$ is the characteristic length of the system and provides a limit to the characteristic length of the particulate phase.

The relative fluctuating velocity is given by

$$u'_r = u'_g - u'_p \quad (22)$$

and

$$|u'_r| = \sqrt{\overline{u'^2_g} - 2\overline{u'_g u'_p} + \overline{u'^2_p}} = \sqrt{\frac{2}{3}(k_g - 2k_{gp} + k_p)} \quad (23)$$

## Numerical Procedure

All the transport equations are discretized using a finite volume formulation in a generalized coordinate space, with metric information expressed in terms of area vectors. The equations are solved on a nonstaggered grid system, wherein all primitive variables are stored at the centroids of the mass control volumes. Third-order quick scheme is used to approximate the convective terms, while second-order accurate central difference scheme is adopted for the diffusion terms. The velocity correction is realized to satisfy continuity through simple algorithm, which couples velocity and pressure. At the inlet boundary the particulate phase velocity is taken to be the same as the gas velocity. The concentration of the particulate phase is set to be uniform at the inlet. At the outlet the zero streamwise gradients are used for all variables. The wall boundary conditions are based on the model of Tu and Fletcher.[16]

All the governing equations for both the carrier and dispersed phases are solved sequentially at each iteration, the solution process is started by solving the momentum equations for the gas phase followed by the pressure-correction through the continuity equation, turbulence equations for the gas phase, are solved in succession. While the solution process for the particle phase starts by the solution of momentum equations followed by the concentration then gas-particle turbulence interaction to reflect the two-way coupling, the process ends by the solution of turbulence equation for the particulate phase. At each global iteration, each equation is iterated, typically 3 to 5 times, using a strongly implicit procedure (SIP). The earlier solution process is marched toward a steady state, and is repeated until a converged solution is obtained. The independency of grid over the converged solution was checked by refining the mesh system through doubling the number of grid points along the streamwise and the lateral directions. Simulations results revealed that the difference of the reattachment length between the two mesh schemes is less than 3%.

## Code Verification

In this section the code is validated for mean streamwise velocities and fluctuations for both the carrier and dispersed phases against the benchmark experimental data of Fessler and Eaton.[6] This task is undertaken to verify the fact that these two classes of particles, which share the same Stokes number, but varied particle Reynolds number can be handled by the code. Figure 1 show the backward-facing step geometry used in this study, which is similar to the one used in the experiments of Fessler and Eaton,[6] which has got a step height (h) of 26.7 mm. As the span wise z-direction perpendicular to the paper is much larger than the y-direction used in the experiments, the flow is considered to be essentially two-dimensional (2-D). The backward-facing step has an expansion ratio of 5:3. The Reynolds number over the step works out to be 18,400 calculated based on the centerline velocity and step height (h).

*Mean Streamwise Velocities.* The mean streamwise velocities for the gas phase have been shown in Figure 2 for various stations along the backward-facing step geometry, it can be generally seen that there is fairly good agreement with experimental findings of Fessler and Eaton.[6] This is then followed by the streamwise velocities for the two classes of particles considered in this study, whose properties

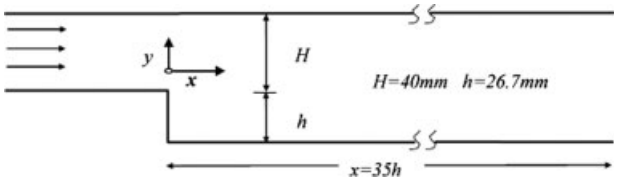


**Figure 1. Backward facing step geometry.**

**Table 1. Properties of the Dispersed Phase**

| | | |
|---|---|---|
| Nominal Diameter ($\mu$m) | 150 | 70 |
| Material | Glass | Copper |
| Density (kg/m$^3$) | 2500 | 8800 |
| Stokes Number ($St$) | 7.4 | 7.1 |
| Particle Reynolds number ($Re_p$) | 9.0 | 4.0 |

are tabulated in Table 1. The broad varying characteristics of different particle sizes and material properties can be unified by a single dimensionless parameter; it is also used to quantify the particles responsivity to fluid motions, and this nondimensional parameter is the Stokes number and is given by the ratio of particle relaxation time to time that of the appropriate fluid time scale $St = t_p/t_s$. In choosing the appropriate fluid time scale, the reattachment length has not been considered as it varies due to addition of particles and is not constant in this study, rather a constant length scale of five step heights, which is in accordance to the reattachment length is used. The resulting time scale is given by $t_s = 5h/U_o$, in accordance with the experiments of Fessler and Eaton.[6]

The significance of the Stokes number is that a particle with a small Stokes number ($St \ll 1$) are found to be in near velocity equilibrium with the surrounding carrier fluid, there by making them extremely responsive to fluid velocity fluctuations, in fact laser doppler velocimetry (LDV) takes advantage of this to deduce local fluid velocity from the measured velocity of these very small Stokes number particles, however, on the other hand for a larger Stokes number ($St \gg 1$) particles are found be no longer in equilibrium with the surrounding fluid phase as they are unresponsive to fluid velocity fluctuations, and they will pass unaffected through eddies and other flow structures.

Figure 3a and b shows the mean streamwise velocity profiles for the two particle classes considered in this study, it can be seen that there is generally a fairly good agreement with the experimental results. From the particle mean velocity graphs of the carrier and dispersed phases it can be inferred, that the particle streamwise velocity at the first station x/h = 2 is lower than the corresponding gas velocities, this is in lines with the fully developed channel flow reaching the step as described in the experiments of Kulick et al.,[24] wherein the particles at the channel centerline have lower streamwise velocities than that of the fluid as a result of cross-stream mixing. However, the gas velocity lags behind the particle velocities aft of the sudden expansion as the particles inertia makes them slower to respond to the adverse pressure gradient than the fluid.

*Mean Streamwise Fluctuations.* The code has been further validated for mean streamwise fluctuations and Figure 4 shows the mean streamwise fluctuations for the gas phase against the experimental data. It is seen that there is a general under prediction of the simulated data with the experimental results, and this is more pronounced toward the lower wall for a height of up to y/h $\leq$ 2, however, the pattern of

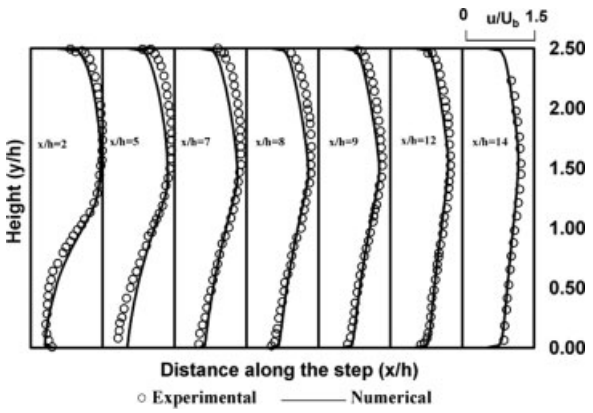


**Figure 2. Mean streamwise gas velocities.**

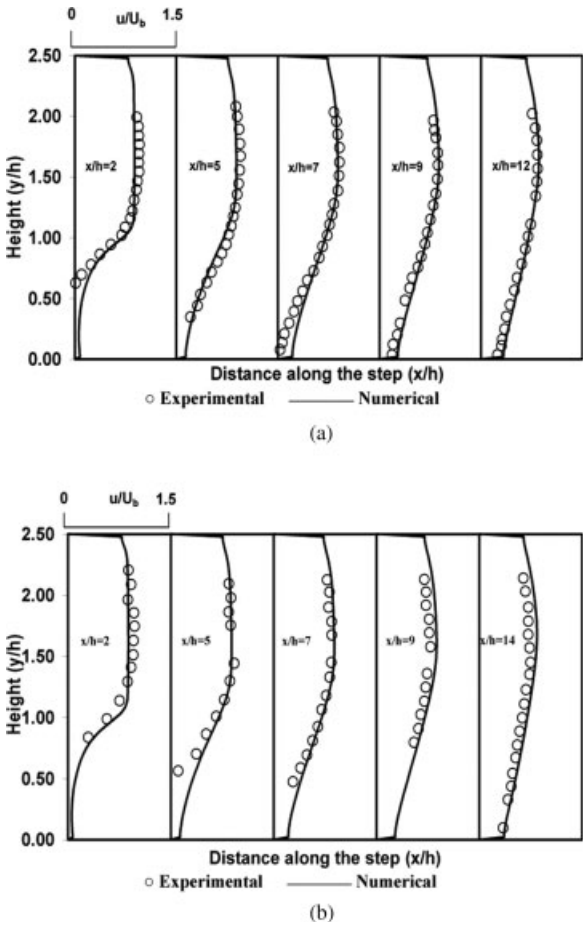


**Figure 3. (a) Streamwise mean velocity for 70 $\mu$m copper particles; (b) streamwise mean velocity for 150 $\mu$m glass particles.**

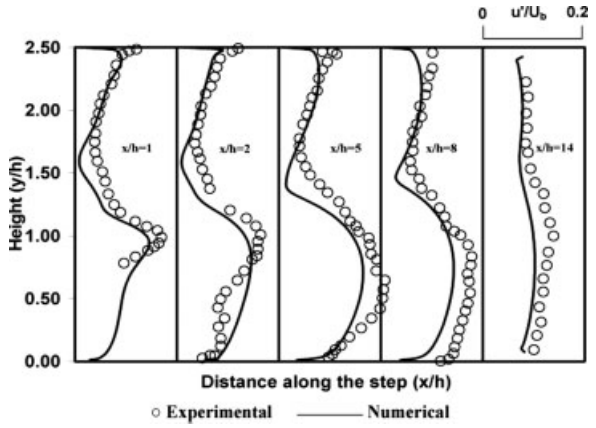


**Figure 4. Fluctuating streamwise gas velocities.**

the simulated results have been found to be in tune with its experimental counterpart.

Figure 5a and b show the streamwise fluctuating particle velocities for the two different classes of particles considered, there has been a minor underprediction until stations $y/h \leq 1$, over all a reasonably good agreement can be observed. It can be also seen that for $y/h > 1.5$, the particle fluctuating velocities are considerably larger than those of the fluid. This again is in accordance with channel flow inlet conditions, wherein the particles have higher fluctuating velocities than those of the fluid owing to cross-stream mixing. All the experimental results used for comparison of particle fluctuating velocities correspond to maximum mass loadings of particles as reported in the experiments of Fessler and Eaton.[4]

## Results and Discussion

*Turbulence Modification.* The plot depicted in the following sections to represent the turbulent modification of the carrier gas phase is given by the ratio of the laden flow r.m.s streamwise velocity to the unladen r.m.s streamwise velocity. These plots signify that any turbulence modification felt in the carrier phase is reflected as an exit of the ratio from unity. The experimental values for the modulation are plotted with error bars, as significant scatter are apparent in these plots, thereby making any variations on the order of $\pm 5\%$ insignificant.[6]

*Analysis of Experimental Data.* As mentioned in the outline, plots 6 and 7 depict the experimental data as obtained from the experiments of Fessler and Eaton.[6] Figure 6a and b represent the mean streamwise particle velocities and fluctuations respectively for the two sets of dispersed phase particles i.e., copper and the glass particles. It can be well seen that the mean velocities and to a similar extent the fluctuations for these two classes seem to behave analogous to each other. However from Figure 7a–c, which shows the experimental TM for the carrier phase in the presence of the dispersed phase at the same mass loading of 40% seem to behave in contrary to the aforementioned findings. In all these stations considered in this study the glass particle seems to attenuate the carrier phase more than copper particles. It is also be seen at the station $x/h = 2$, the attenuation of the turbulence for glass particle is totally opposite in relation to copper particle for location $y/h > 1.25$. At station $x/h = 7$ for certain regions along the height of the step the turbulence attenuation for the two particle classes seems to be in phase, whereas before and after this small region of unison the glass particle seem to attenuate more than the copper particles. At the station $x/h = 14$, it can be clearly seen, that there is a uniform degree of difference in attenuation all along the step, this is more attributed to the uniform distribution of the particles seen along the step.

The maximum turbulence attenuation can be seen for the 150 $\mu$m particles, which is up to 35% as reported from the experiments of Fessler and Eaton,[5] further from the same experiments, TM for varying particle mass loadings have also been tabulated for the two set of particles considered in our study and their TM have found to increase with the increase in mass loadings, and this is attributed mainly due to inherent transfer of turbulent kinetic energy from the gas phase onto the particles, there by causing further more TM of the carrier gas phase.

From the aforementioned analysis, it is quite clear that particles with the same Stokes number modulate the carrier phase turbulence in a totally different fashion. This makes us conclude that although Stokes number can be generalized to account for mean values of velocity and fluctuations, it can-

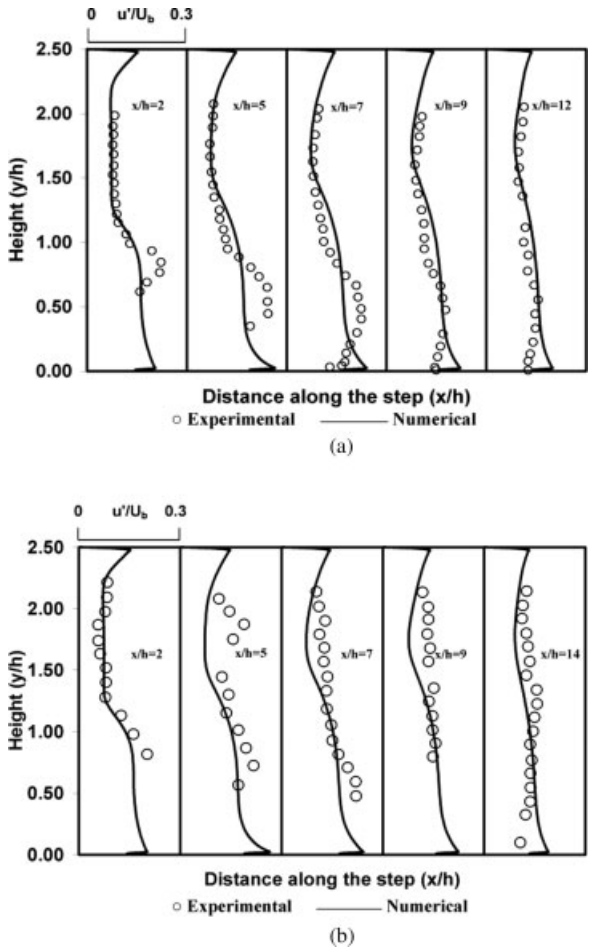


**Figure 5. (a) Fluctuating streamwise particle velocities for 70 $\mu$m copper particles; (b) fluctuating streamwise particle velocities for 150 $\mu$m glass particles.**

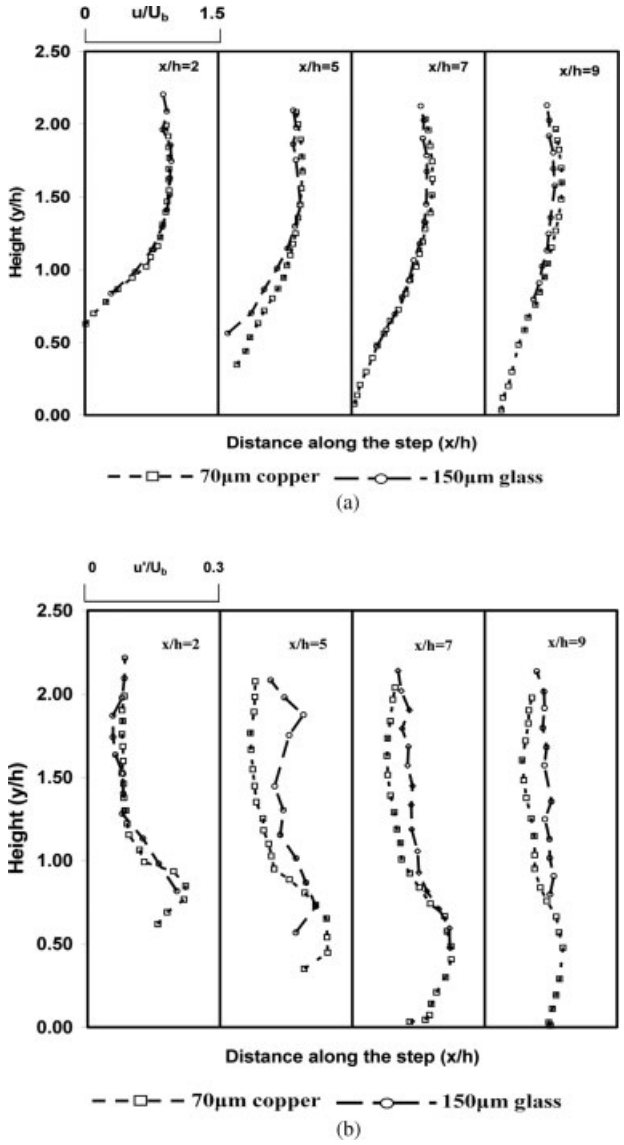


**Figure 6. (a) Experimental mean streamwise particle velocity; (b) experimental fluctuating streamwise particle velocity.**

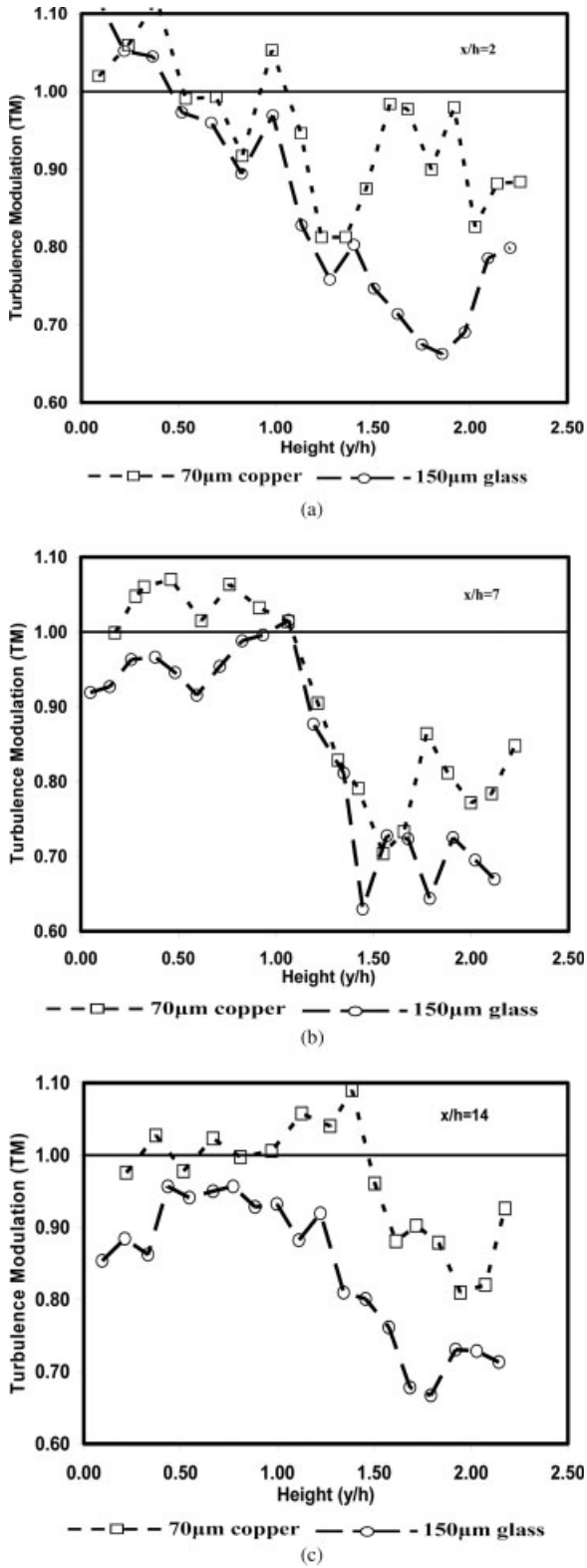


**Figure 7. (a) Experimental turbulence modulation at x/h = 2; (b) experimental turbulence modulation at x/h = 7; (c) experimental turbulence modulation at x/h = 14.**

not be generalized when it comes to TM, in which case something more than Stokes number is required to define one's particle response to surrounding carrier phase turbulence either to attenuate or enhance it.

*Testing of Different TM Models.* Herein, our current formulation of turbulence modeling outlined earlier is tested and compared against the published TM models, in these models the turbulent length scale of the gas phase has been suitably altered to take in account the presence of the particles in the gas phase. Kenning and Crowe[18] stated that if the concentration of particles introduced into a flow yields an average interparticle spacing smaller than the inherent dissipation length scale, then the particles may interfere with the existing eddies breaking them up such that the new dissipation length scale is proportional to the average interparticle

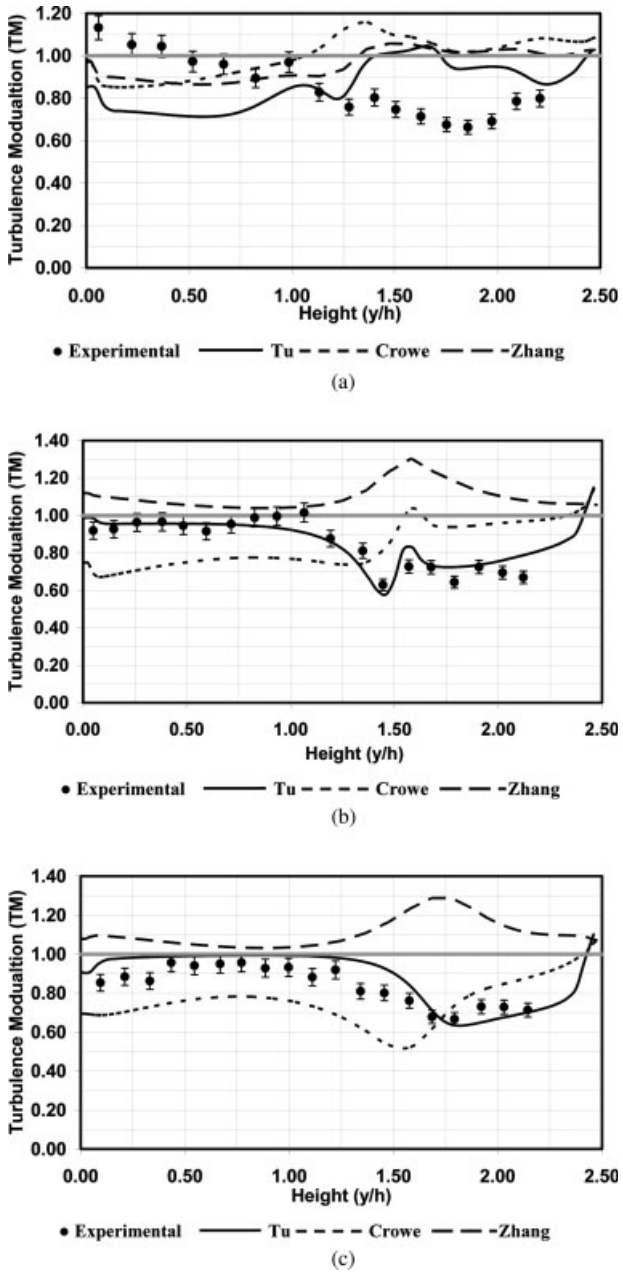


**Figure 8. (a) Turbulence modulation with various models for 150 $\mu$m glass particles at x/h = 2; (b) turbulence modulation with various models for 150 $\mu$m glass particles at x/h = 7; (c) turbulence modulation with various models for 150 $\mu$m glass particles at x/h = 14.**

spacing rather than the geometry of the pipe or jet. Based on this analysis, a hybrid length scale ($l_h$), dependent on both the inherent dissipation length scale ($l_i$) and the average interparticle spacing ($\lambda/d$) was put forward, where $l_h = \frac{2l_i\lambda}{l_i+\lambda}$ and $\lambda/d \approx (\pi/6\varepsilon_d)^{1/3} - 1$. In the limit of two scales $l_i$ and $\lambda$, being equal, there is no change in length scale, and if they are not equal the hybrid length scale will fall between them.

Zhang and Reese[19] proposed a new model wherein the turbulent length scale $l$ can be determined by a new relation to the turbulent energy dissipation rate $\varepsilon$ to account for the effect of the interparticle length scale. They consider the turbulent length scale analogous to the free path of the random motion of gas molecules. As the space occupied by the spherical particles is not available to the gas molecular clusters, and the gas turbulence is likely to be negligible at solid-volume fractions even somewhat below the closely packing limit, the reduced turbulent length scale $l_r$, is given by $l_r = [1 - (\frac{6\varepsilon_d}{\pi\varepsilon_{2m}})^{1/3}]l$, where $\varepsilon_{2m}$ represents the random close-packing particle-volume fraction, which is 0.64. The new relation between turbulent energy dissipation rate and turbulent length scale becomes $\varepsilon = (C_\mu^{3/4}/(1 - (6\varepsilon_2/\pi\varepsilon_{2m})^{1/3}))k^{3/2}/l$.

The combined results for three turbulent modification models are depicted in the plots 8a–c, for the glass particle. It can be seen that our proposed model seem to better represent the turbulent modulation effects in the gas phase in comparison to the two other models of Kenning and Crowe[18] and Zhang and Resse.[19] It can be seen that there is a general over prediction using the Zhang's model and a mixed behavior for the Kenning and Crowe's model along the step, for the two classes of particles considered, however, maximum under prediction for the Crowe model is found at the exit for the copper particles. The results of the other two models tested seem not to fair well, due to the fact that these two models have been tested for the simple flow field, i.e., vertical gas-particle flows.

*Extended TM and PND Results.* In this section we have tried to derive an understanding for the TM of the carrier gas phase in the presence of particles using our turbulent formulation, along with its corresponding PND results for the two classes we have considered in this study, the simulated results of the aforementioned two parameters are plotted along side the experimental findings of Fessler and Eaton.[6]

Figure 9a–c shows the combined numerical and experimental results of TM (secondary axis) and PND (primary axis) for three sections along the step viz. x/H = 2, 7 and 14 for copper particles. It can be noted at station x/h = 2 just aft of the step, for y/h < 1 there exist very few particles, but, however, the experimental TM shows a wavy behavior in comparison to the simulated results, which seem to behave in unison with the PND, however aft of this section, the simulated values compare well with the experimental data. In the middle of the step at station x/h = 7, there is generally a good comparison of the experimental and simulated values for both the TM and PND. At the exit (x/h = 14) however, there seems to be general under prediction of TM for y/h > 1.5, while the PND seem to vary from underpredicting to over predicting the experimental data. Figures 10a–c shows plots of the glass particles for the same three sections along the step. At section x/h = 2, the simulated values seem to over predict the experimental data for y/h > 1, however this distinct behavior of maximum attenuation as reported by Fessler and Eaton[6] occurs here, this under prediction is not quite in terms with the PND results which seem to show a uniform distribution. A reasonably good agreement is with both turbulence modification and PND can be seen for stations x/h = 7 and 14.

It is generally seen that for the two classes of particles considered, there exist considerably more particles in the region y/h > 1 for locations x/h = 2 and 7, and the particles exhibit a uniform distribution by the time it reaches the location x/h = 14 due to its uniform spreading action, but despite a uniform distribution, the turbulence attenuation is still

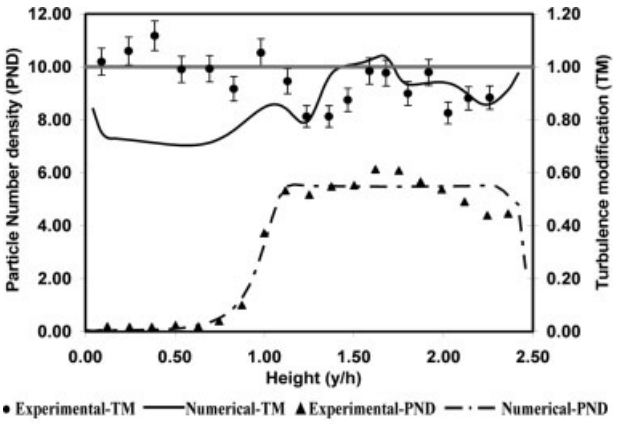


(a)

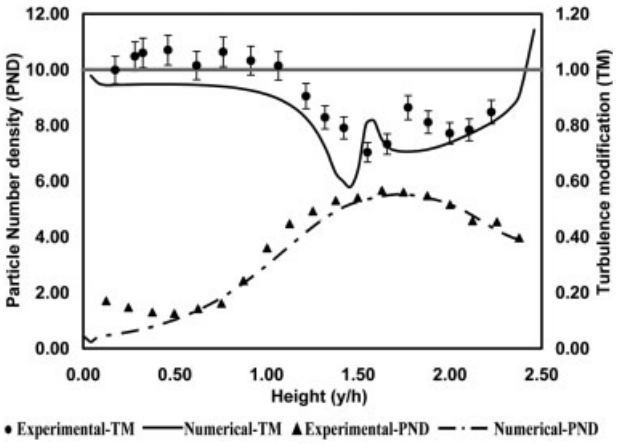


(b)

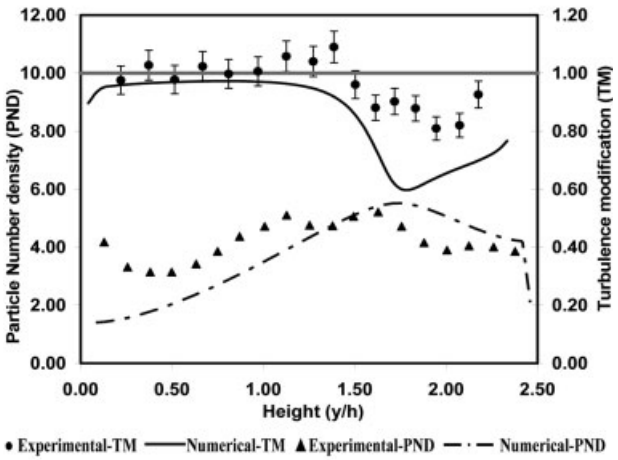


(c)

**Figure 9. (a) Turbulence modulation and particle number density for 70 $\mu$m copper particles at x/h = 2; (b) turbulence modulation and particle number density for 70 $\mu$m copper particles at x/h = 7; (c) turbulence modulation and particle number density for 70 $\mu$m copper particles at x/h = 14.**

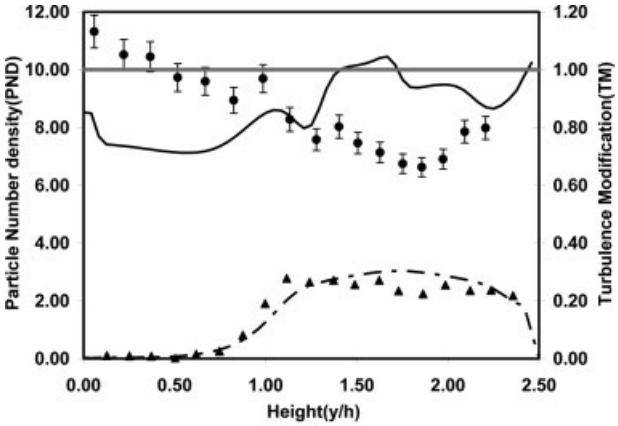


(a)

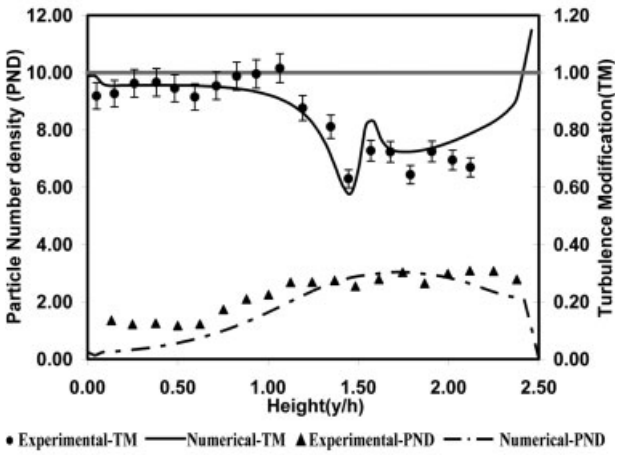


(b)

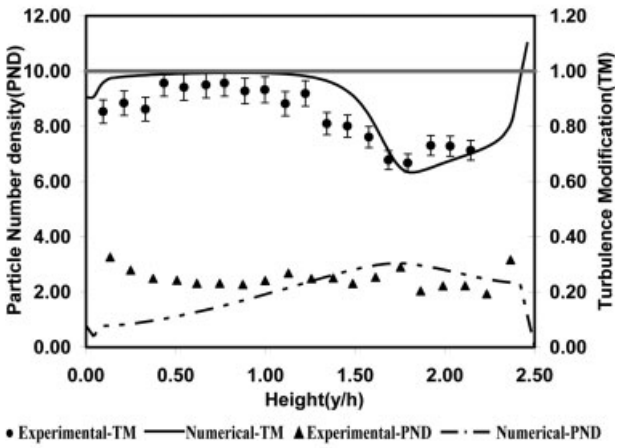


(c)

**Figure 10. (a) Turbulence modulation and particle number density for 150 $\mu$m glass particles at x/h = 2; (b) turbulence modulation and particle number density for 150 $\mu$m glass particles at x/h = 7; (c) turbulence modulation and particle number density for 150 $\mu$m glass particles at x/h = 14.**

small for y/h < 1 at the x/h = 14, and this is attributed to the noneffectiveness of the particles to large scale vortices, which are reported to exist downstream of the single phase backward facing step.[25] From the PND results for the two classes of particles, both simulated and experimental plots show that there exists very few particles in the region y/h<1 before the reattachment point and a significant spreading has taken place by, at locations x/h = 9 and 14, considering this behavior alongside with the turbulence attenuation, one can state that lack of turbulence modulation is not simple due to the absence of particles, but clearly a difference on response of the turbulence in a specific region due to the presence of particles,[6] and this has been explicitly seen in our simulated values using our turbulence formulation mentioned in the previous section.

*TM and Particle Reynolds Number.* In this section, we have tried to explain the phenomenon of the carrier phase TM by particles in relation to particle Reynolds number ($Re_p$). Looking back at Table 1, it is seen that for the glass particles the $Re_p$ is almost 125% more than for the copper particles and also considering the size of the particles which is around 114% more for the glass particles in comparison to the copper particles. The presented results on the degree of carrier phase turbulence attenuation also seem to throw some interesting pattern especially in regards to copper and glass particles, which almost share the same Stokes number. Based on this similarity one would expect that their response to the turbulence be the same, although this fact seems to be quite in lines with the particle mean and fluctuating velocities, but their behavior in regards to turbulence modification paint a totally different picture, which makes us conclude that the turbulence attenuation has a direct link of the particles onto the turbulence rather a derived effect on the mean flow modifications.[4] And this attenuation cannot follow suit with increasing loading and particle size as there will be an increase in the turbulence as reported by Hetsroni,[5] it is also interesting to note from the same author that apart from the Stokes number, particle Reynolds number plays an important role in the systematic behavior of the particles, the same has been reported from the experimental findings of Fessler and Eaton,[6] this is in conformity to our simulated results, wherein the two classes of copper and glass behave differently although their particle Stokes number remain the same.

It is known from previous studies that there is a physical increase in the carrier phase turbulence and this is attributed to the wake formation behind these large particles similar to the ones behind the cylinders encountered in single phase flows. Experimental studies from Eaton et al.[26] state that for $Re_p$ around 10, the modulation is caused due to the strong asymmetric wake distortion extending many particle diameters downstream, whereas for $Re_p$=1, the flow distortion is highly localized to a nearly symmetric region extending only a few particle diameters. Taking this into consideration one would expect a significant enhancement of the carrier phase turbulence for the glass particles, but in contrast significant attenuation have taken place, the maximum attenuation is noted at location x/h = 2, and the attenuation of glass particles is roughly about 44% more than its counterpart copper particles. This behavior of the glass particle to attenuate rather than enhance the turbulence of the carrier phase can be explained by the fact that, due to strong asymmetric wake, the distortion caused by this class of particles is dissipated more easily within the carrier gas phase, this is in sharp contrast to the parallel experiments run by Sato et al.[20] using water as the carrier phase fluid, although similar Stokes number were achieved, much higher $Re_p$ was realized, this in total showed significant vortices behind the particle and also an enhancement in the carrier phase turbulence, which is primarily caused due to the different density ratios between the carrier and dispersed phases, which makes one to justify that Stokes number alone will not be able to describe the parameter space of the dispersed two-phase flow problems, $Re_p$ should also be taken into consideration.

## Conclusion

Particle-turbulence two-phase flow interaction has been successfully investigated with the Eulerian two-fluid model. The numerical code has been validated against the experimental results of Fessler and Eaton[6] for mean velocity, and the fluctuating velocities for both carrier phase and the dispersed particulate phase. The current numerical exploration of TM, wherein two sets of particles sharing the same Stokes number, but quite different particle Reynolds number for a shear flow geometry like backward-facing step have been unique and one of the first in its class, as there is no current published numerical work, comparing the same against any experimental data. The majority of the results agree reasonably well with the experimental data; however, there have been some discrepancies felt at the proximity of the experimental results, at this stage. Further insight into the same will be carried out in a systematic manner, there by to improve the current model, to reflect better prediction.

The carrier phase turbulence modulation for these two classes of particles have been studied along the three sections that is near the inlet (x/h = 2), in the midsection (x/h = 7) and just aft of the exit (x/h = 14). Our current formulation of turbulence modeling incorporating the solution of additional equations has been tested against the other published turbulent modification models (Kenning and Crowe[18]; Zhang and Reese[19]), and it is felt that our formulation seem to better represent the TM behavior. It is also been shown that the TM is not merely due to the presence of particles rather than its response to the turbulent structures. It can also be concluded that even though the 70 $\mu$m copper and 150 $\mu$m glass particles share the same Stokes number, their behavior seems to be quite different, which suggests that Stokes number alone does not characterize the particle behavior, thereby, making particle Reynolds number an important parameter in classifying the way the particles behave.


## Acknowledgement

The first author was supported by International Postgraduate Research Scholarship (IPRS) for his graduate study.


## Notation

$B_{gp}$, $B_\varepsilon$ = model constants for the Eulerian two-fluid model
$C_\mu$ = coefficient in the RNG $k$-$\varepsilon$ turbulence model
$C_D$ = particle-drag coefficient
$C_{\varepsilon 1}$, $C_{\varepsilon 2}$ = model constants for standard and RNG $\kappa$-$\varepsilon$ turbulence models
$D$ = characteristic length (100 mm)
$d_p$ = particle diameter

$f$ = correction factor for drag force
$F_{Di}$ = aerodynamic drag force
$F_{Gi}$ = gravity force
$F_{WMi}$ = wall-momentum transfer due to particle-wall collision force
$g$ = gravitational acceleration
$I_{gp}$ = turbulence interaction between the gas and particle phases for the particle phase turbulent fluctuating energy
$l$ = length scale of energetic turbulent eddies
$m$ = ratio of mean bulk particle to gas density
$n$ = ration of gas to particulate density
$P_{kgp}$ = turbulence production by the mean velocity gradients of two phases
$P_{kp}$ = production term of the particle fluctuating energy
$PND$ = particle number density
$r$ = uniform random number
$R$ = strain rate
$Re$ = Reynolds number
$S$ = source term
$St$ = Stokes number
$S_{ij}$ = strain rate
$TM$ = Turbulence Modulation
$t_{cross}$ = eddy crossing time
$t_p$ = particle relaxation time
$t_s$ = system response time
$T_L$ = fluid Lagrangian integral time
$u^i$, $u^j$, $u^k$ = velocity
$U_b$ = inlet bulk velocity
$x_i$, $x_j$, $x_k$ = Cartesian coordinate system
$\varepsilon_d$ = volume fraction of the particulate phase

### Greek letters

$\alpha$ = inverse Prandtl number
$\beta$ = model constant for RNG $\kappa$-$\varepsilon$ turbulence model
$\varepsilon$ = dissipation rate of turbulent kinetic energy
$\eta$ = function defined in Eq. (8),
$\eta_o$ = model constant for RNG $\kappa$-$\varepsilon$ turbulence model
$k$ = turbulent kinetic energy
$v$ = kinematic viscosity
$\theta$ = angle between velocities of the particle and gas
$\rho$ = density
$\sigma$ = turbulence Prandtl number
$\zeta$ = normally distributed random number
$\prod_{gp}$ = turbulence interaction between the gas and particle phases for the gas-particle
$\lambda$ = interparticle spacing

### Subscripts

$g$ = gas phase
$gp$ = gas-particle
$h$ = hybrid
$i$ = inherent
$p$ = particle phase
$s$ = solid phase
$l$ = laminar phase
$t$ = turbulent phase

### Superscript

$\underline{(\ )}'$ = fluctuation
$(\quad)$ = Favre-averaged

## Literature Cited


1. Patil DJ, Smit J, Van Sint Annaland M, Kuipers JAM. Wall-to-bed heat transfer in gas-solid bubbling fluidized beds. *AIChE J*. 2006;52:58–74.
2. Elghobashi SE, Truesdell GC. On the Two-way interaction between homogenous turbulence and dispersed solid particles. I: Turbulence modification. *Phys Fluids A*. 1993;5:1790–1801.
3. Gore RA, Crowe CT. Modulation of turbulence by dispersed phase. *J Fluids Engr*. 1991;113:304–307.
4. Fessler JR, Eaton JK. Turbulence modification by particles in a backward-facing step flow. *J Fluid Mech*. 1999;394:97–117.
5. Hetsroni G. Particles-turbulence interaction. *Intl J Multiphase Flow*. 1989;15:735–746.
6. Fessler JR, Eaton JK. *Particle-turbulence interaction in a backward-facing step flow. Mech. Engng Dept. Rep. MD-70*. Stanford University, Stanford, California; 1995.
7. Elghobashi SE, Abou-Arab T. A two-equation model for two-phase flows. *Phys Fluids*. 1983;26:931–938.
8. Sheun JS, Solomon ASP, Zhang QF, Faeth, GM. Structure of particle-laden jets: measurements and perdictions. *AIAA J*. 1985;23:396–404.
9. Mostafa AA, Mongia HC. On the Modelling of turublent evaporating sprays: Eulerian versus Lagrangian approach. *Int J Heat & Mass Tranf*. 1987;30:2583–2593.
10. Chen CP, Wood PE. A Turbulence closure model for dilute gas-particle flows. *Canadian J. Chem Eng*. 1985;63:349.
11. Rizk MA, Elghobashi SE. A two-equation turbulence model for dispersed dilute confined two-phase flows. *Intl J Multiphase Flows*. 1989;15:119–133.
12. Dasgupta S, Jackson R, Sundaresan S. Gas-particle flow in vertical pipes with high mass loading of particles. *Powder Technol*. 1989;96:6–23.
13. Bolio E, Yasuna J, Sinclair J. Dilute turbulent gas-solid flow in risers with particle interactions. *AIChE J*. 1995;41:1375–1388.
14. Zhou LX, Chen T. Simulation of swirling gas-particle flows using USM and k-$\varepsilon$-kp two-phase turbulence models. *Powder Technol*. 2001;114:1–11.
15. Simonin, O. Continuum modelling of dispersed two-phase flows Combustion and Turbulence in Two-phase Flows (*Lecture Series 1996–02*). Rhode Saint Genèse: Von Karman Institute for Fluid Dynamics; 1996.
16. Tu JY, Fletcher CAJ. Numerical computation of turbulent gas-solid particle flow in a 90° Bend. *AIChE J*. 1995;41:2187–2197.
17. Tu JY. Computational of turbulent two-phase flow on overlapped grids. *Numer Heat Transfer Part B*. 1997;32:175–195.
18. Kenning VM, Crowe CT. Effect of particle on carrier phase turbulence in gas-particle flows. *Int J Multiphase Flow*. 1997;23:403–408.
19. Zhang YH, Reese JM. Gas turbulence modulation in a two-fluid model for gas-solid flows. *AIChE J*. 2003;49:3048–3065.
20. Sato Y, Fukuichi V, Hishida K. Effect of inter-particle spacing on turbulence modulation by Lagrangian PIV. *Int J Heat Fluid Flow*. 2000;21:554–561.
21. Schuh MJ, Schuler CA, Humphrey JAC. Numerical calculation of particle-laden gas flows past tubes. *AIChE J*. 1989;35:466–480.
22. Yakhot V, Orszag SA. Renormalization group analysis of turbulence I. basic theory. *J Sci Comput*. 1986;1:3–51.
23. Huang XY, Stock DE, Wang LP. Using the monte-carlo process to simulate two-dimensional heavy particle dispersion. *ASME-FED, Gas-Solid flows*. 1993;166:153–160.
24. Kulick JD, Fessler JR, Eaton JK. Particle response and turbulence modification in fully developed channel flow. *J Fluid Mech*. 1994;277:109–134.
25. Le H, Moin P, Kim J. Direct numerical simulation of turbulent flow over a backward-facing step. *J Fluid Mech*. 1997;330:349–374.
26. Eaton JK, Paris AD, Burton TM. Local distortion of turbulence by dispersed particles. *AIAA Paper*. 1999;99–3643.


*Manuscript received Oct. 17, 2006, and revision received May 16, 2007.*